



HAL
open science

Arrangement of Monofunctional Silane Molecules on Silica Surfaces: Influence of Alkyl Chain Length, Head-Group Charge, and Surface Coverage, from Molecular Dynamics Simulations, X-ray Photoelectron Spectroscopy, and Fourier Transform Infrared Spectroscopy

Solène Lecot, Antonin Lavigne, Zihua Yang, Thomas Gehin, Claude Botella, Vincent Jousseaume, Yann Chevolot, Magali Phaner-Goutorbe, Christelle Yeromonahos

► To cite this version:

Solène Lecot, Antonin Lavigne, Zihua Yang, Thomas Gehin, Claude Botella, et al.. Arrangement of Monofunctional Silane Molecules on Silica Surfaces: Influence of Alkyl Chain Length, Head-Group Charge, and Surface Coverage, from Molecular Dynamics Simulations, X-ray Photoelectron Spectroscopy, and Fourier Transform Infrared Spectroscopy. *Journal of Physical Chemistry C*, 2020, 124 (37), pp.20125-20134. 10.1021/acs.jpcc.0c05349 . hal-03214427

HAL Id: hal-03214427

<https://hal.science/hal-03214427v1>

Submitted on 1 May 2021

HAL is a multi-disciplinary open access archive for the deposit and dissemination of scientific research documents, whether they are published or not. The documents may come from teaching and research institutions in France or abroad, or from public or private research centers.

L'archive ouverte pluridisciplinaire **HAL**, est destinée au dépôt et à la diffusion de documents scientifiques de niveau recherche, publiés ou non, émanant des établissements d'enseignement et de recherche français ou étrangers, des laboratoires publics ou privés.

C: Surfaces, Interfaces, Porous Materials, and Catalysis

Arrangement of Monofunctional Silane Molecules on Silica Surfaces: Influence of the Alkyl Chain Length, Head-Group Charge and Surface Coverage, from Molecular Dynamics Simulations, X-Ray Photoelectron Spectroscopy and Fourier Transform Infrared Spectroscopy Analysis.

Solène Lecot, Antonin Lavigne, Zihua Yang, Thomas Géhin, Claude Botella, Vincent Jousseume, Yann Chevotot, Magali Phaner-Goutorbe, and Christelle Yeromonahos

J. Phys. Chem. C, **Just Accepted Manuscript** • DOI: 10.1021/acs.jpcc.0c05349 • Publication Date (Web): 21 Aug 2020

Downloaded from pubs.acs.org on August 25, 2020

Just Accepted

“Just Accepted” manuscripts have been peer-reviewed and accepted for publication. They are posted online prior to technical editing, formatting for publication and author proofing. The American Chemical Society provides “Just Accepted” as a service to the research community to expedite the dissemination of scientific material as soon as possible after acceptance. “Just Accepted” manuscripts appear in full in PDF format accompanied by an HTML abstract. “Just Accepted” manuscripts have been fully peer reviewed, but should not be considered the official version of record. They are citable by the Digital Object Identifier (DOI®). “Just Accepted” is an optional service offered to authors. Therefore, the “Just Accepted” Web site may not include all articles that will be published in the journal. After a manuscript is technically edited and formatted, it will be removed from the “Just Accepted” Web site and published as an ASAP article. Note that technical editing may introduce minor changes to the manuscript text and/or graphics which could affect content, and all legal disclaimers and ethical guidelines that apply to the journal pertain. ACS cannot be held responsible for errors or consequences arising from the use of information contained in these “Just Accepted” manuscripts.

1
2
3
4
5
6
7 Arrangement of Monofunctional Silane Molecules
8
9
10
11 on Silica Surfaces: Influence of the Alkyl Chain
12
13
14
15 Length, Head-Group Charge and Surface Coverage,
16
17
18
19 from Molecular Dynamics Simulations, X-Ray
20
21
22
23 Photoelectron Spectroscopy and Fourier Transform
24
25
26
27 Infrared Spectroscopy Analysis.
28
29
30
31
32

33 *Solène Lecot[§], Antonin Lavigne[§], Zihua Yang[§], Thomas Géhin[§], Claude Botella[§], Vincent*
34 *Jousseaume[⊥], Yann Chevolot[§], Magali Phaner-Goutorbe[§], Christelle Yeromonahos^{§*}*
35
36
37

38
39 [§] Université de Lyon, Institut des Nanotechnologies de Lyon UMR 5270, Ecole Centrale de
40
41 Lyon, 36 avenue Guy de Collongue, 69134 Ecully, France
42
43

44 [⊥] Université Grenoble Alpes, CEA, LETI, F-38000 Grenoble, France
45
46
47
48
49
50
51

52 *** Corresponding Author**
53

54 Christelle Yeromonahos: christelle.yeromonahos@ec-lyon.fr, + 33 4 72 18 62 35
55
56
57
58
59
60

1
2
3 ABSTRACT
4
5
6

7 Surface chemical functionalization is used in analytical tools to immobilize biomolecules that will
8 capture a specific analyte, but also to reduce the nonspecific adsorption. Silane monolayers are
9 widely used to functionalize silica surfaces. Their interfacial properties are linked to the silane
10 organization. Here we study, by Molecular Dynamics simulations, the effects of silane molecule
11 headgroup charge, alkyl chain length, and surface coverage on the structure of silane monolayers.
12
13 Four molecules are investigated: 3-aminopropyltrimethoxysilane, n-
14 propyltrimethylmethoxysilane, octadecyltrimethylmethoxysilane, tert-butyl-11-
15 (dimethylamino(dimethyl)silyl)undecanoate. The results suggest that, while long alkyl chains
16 straighten out and adopt a more organized structure as surface coverage increases, the tilt angle of
17 short chains is independent from surface coverage. Furthermore, in the case of long alkyl chains,
18 a charged headgroup seems to reduce the tilt angle to surface coverage dependence. The simulated
19 alkyl chain tilt angles were qualitatively validated by infrared spectroscopy and X-ray
20 photoelectron spectroscopy. Also, a hexagonal packing is observed in all the monolayers, but is
21 more defined as surface coverage increases. The nematic order parameter suggests that this
22 packing is governed by the parallel orientation of the first C-C bonds near the surface. So, even
23 short alkyl chains, with a large tilt angle distribution, present a hexagonal packing.
24
25
26
27
28
29
30
31
32
33
34
35
36
37
38
39
40
41
42
43
44
45
46
47
48
49
50
51
52
53
54
55
56
57
58
59
60

Introduction

A large number of applications takes advantage of surface chemical functionalization. In particular, in the field of biosensing, the specificity of the device (the fact of capturing solely a given analyte) and the signal to noise ratio are related to surface chemistry. For example, surface chemical functionalization allows the immobilization of biomolecules that will capture specifically biomarkers (peptides, proteins, DNA) or whole organisms for diagnosis purposes.¹⁻⁶ The background signal can also be reduced thanks to the chemical functionalization of material surfaces allowing the reduction of non-specific adsorption. Among the various chemical functionalizations, silane molecules have been widely used for the modification of oxides, especially oxidized silicon surfaces (SiO₂).^{2,3,7-9}

The structure, organization and surface energies of various silane modified SiO₂ surfaces have been studied by various characterization techniques as a function of experimental parameters, in particular in the case of multifunctional silane monolayers. Atomic Force Microscopy (AFM) experiments suggested that, after deposition on SiO₂ surface, silane molecules can diffuse laterally to self-assemble either into fractal network or into liquid phase state, depending on external parameters such as temperature.¹⁰ Also, AFM studies have established that the strength of hydrophobic interactions on a silane monolayer is strongly related to the order of the silane molecules.¹¹ Indeed, pull-off forces resulting from hydrophobic adhesion are higher on crystalline-like monolayers than on liquid-like monolayers. The structure of *n*-alkane monolayers, with *n* > 12, has been extensively studied by Fourier Transform Infra-Red (FTIR) and X-Ray Diffraction (XRD) measurements.¹²⁻¹⁷ While the positions of the methyl and methylene vibration modes from FTIR spectra yielded information on the presence of gauche defects in the alkyl chains and on the average alkyl chain tilt angle, the molecule crystalline packing inside the monolayer was addressed

1
2
3 by XRD measurements. Hexagonal crystalline-like domains with an intermolecular in-plane
4 distance of 4.7-5 Å were observed for monolayers of *n*-alkylsilane molecules with $n > 14$.^{13,16}
5
6 Shorter *n*-alkylsilane monolayers were shown to present more gauche defects than the longer ones,
7
8 but also a lower surface coverage.¹² Also, in the case of multifunctional silane molecules, a
9
10 Multiple Transmission and Reflection Infra-Red Spectroscopy study shown that the nature of the
11
12 leaving groups (Si(OMe)₃, Si(OEt)₃, Si(Cl)₃) controls the rate of their hydrolysis, leading to very
13
14 different monolayer structures.¹⁷
15
16
17
18
19

20 As the surface coverage cannot easily be varied experimentally, Molecular Dynamics (MD)
21
22 simulations are well suited to study the combined effects of surface coverage and alkyl chain length
23
24 of silane molecules on alkyl chain tilt angle, gauche defects and nematic order parameter.
25
26 However, only few MD simulations studies have addressed these questions. Different MD studies
27
28 suggested that the order parameter of *n*-alkylsilane monolayers (for $n > 8$) increases as the alkyl
29
30 chain length and the surface coverage increase, while alkyl chain tilt angles are independent of
31
32 chain length and decrease as surface coverage increases.¹⁸⁻²² Among them, it was also shown that
33
34 perfluorodecyltrichlorosilane (FDTS) monolayers at high surface coverage present a hexagonal
35
36 packing, whereas such packing was attenuated for octadecyltrichlorosilane (OTS) monolayers for
37
38 the same surface coverage.¹⁸ In the present study, we demonstrate an effect of the head-group
39
40 charge and alkyl chain length ($n < 18$), on the organization of the monolayer.
41
42
43
44
45

46 We propose a MD simulation study on the effects of head-group charge (positive, neutral and
47
48 negative), alkyl chain length (n from 3 to 18), and surface coverage (1.5 to 4.2 nm⁻²) on the
49
50 structure of silane monolayers. The four different silane molecules are 3-
51
52 aminopropyldimethylethoxysilane (C₇H₁₉NOSi named NH₃⁺), n-propyldimethylmethoxysilane
53
54 (C₆H₁₆OSi named CH₃ short), octadecyldimethylmethoxysilane (C₂₁H₄₆OSi named CH₃ long), and
55
56
57
58
59
60

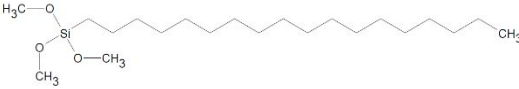
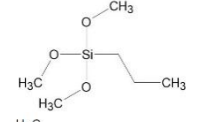
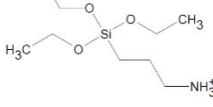
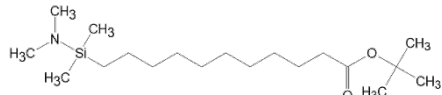
1
2
3 tert-butyl-11-(dimethylamino(dimethyl)silyl)undecanoate ($C_{19}H_{41}NO_2Si$, leading to COO^- after
4 deprotection) (Table 1). The different silane monolayers were characterized by the alkyl chain tilt
5 angle, the average number of gauche defects in the alkyl chains, the nematic order parameter for
6 each C-C bond and its overall distribution, and the hexagonal packing of silane molecules on SiO_2
7 surface and its persistence length. To check that the simulated morphologies were consistent with
8 experimental evidences, alkyl chain tilt angles were compared to experimental values obtained
9 from FTIR-Attenuated Total Reflectance (FTIR-ATR) measurements. To this aim, four silane
10 monolayers (one per silane molecule type) were elaborated from a liquid phase process on SiO_2
11 surfaces. The surface coverages were estimated by X-ray Photoelectron Spectroscopy (XPS)
12 analysis.
13
14
15
16
17
18
19
20
21
22
23
24
25
26

27 **1. Materials and methods**

28 *1-1. Experimental materials and methods*

29
30
31
32
33 **Materials.** SiO_2 (20 nm) / Aluminium (200 nm) / Silicon substrates were prepared by Physical
34 Vapor Deposition (PVD) using a 200 mm Applied Materials Endura 5500 platform. The
35 depositions were performed on Si (100) wafers without air break between Aluminium and SiO_2 .
36 3-aminopropyldimethylethoxysilane 95% (NH_3^+), n-propyldimethylmethoxysilane 95% (CH_3
37 short) and octadecyldimethylmethoxysilane 95% (CH_3 long) were purchased from ABCR. Tert-
38 butyl-11-(dimethylamino(dimethyl)silyl)undecanoate (leading to COO^- after deprotection) was
39 synthesized accordingly to a protocol previously reported.²³ The chemical structures of the four
40 molecules are shown in Table 1.
41
42
43
44
45
46
47
48
49
50
51
52
53
54
55
56
57
58
59
60

Table 1. The different silane molecules and surface coverage studied.

Designation of silane molecule	Silane structural formula	Surface coverage used in MD simulations (nm ⁻²)	Surface coverage estimated by XPS analysis (nm ⁻²)
Systems with silane layer	CH ₃ long 	1.5 – 3.0 – 4.2	3
	CH ₃ short 	1.5 – 3.0 – 4.2	3
	NH ₃ ⁺ 	3.0	8
	COO ⁻ 	3.0 – 4.2	3
System without silane layer	Bare SiO ₂		

Chemical surface functionalization. The substrates were cleaned by ozone/Ultraviolet treatment under oxygen flow for 30 min to remove organic contamination and to obtain a hydroxyl-terminated surface. Next, the substrates were heated at 150°C for 4 hours under nitrogen, allowed to cool to room temperature under nitrogen and then, the substrates were immersed in 10 ml dried pentane containing 90 µl of silane molecules. After 1 hour of incubation, the pentane was evaporated and the samples were heated at 150°C for 15 hours, to allow the silanization reaction. Finally, the samples were washed 10 minutes in tetrahydrofuran (THF) under sonication, and 10 minutes in ultrapure water under sonication.

1
2
3 **XPS analysis.** XPS measurements were performed using a VSW spectrometer equipped with a
4 monochromatized X-ray source (Al K α 1486.6 eV) in which the angle between the incident beam
5 and the detector was the magic angle. The angular resolution was 3°. Take-off angle was 90°
6 relative to the substrate surface. The energetic resolution was 0.2 eV. The data analysis was
7 performed with CasaXPS software. Si(-O)₄ binding energy was set at 104 eV. A Shirley
8 background was subtracted on Si2p and O1s spectra when coming from bulk elements while a
9 linear background was subtracted on C1s spectra as surface elements. Peaks were fitted by a Gauss-
10 Lorentz curve.
11
12
13
14
15
16
17
18
19
20
21

22 **FTIR-ATR analysis.** FTIR-ATR was performed using a Thermo Nicolet 6700 spectrometer with
23 a Mercury-Cadmium-Telluride (MCT) detector and a diamond crystal from 800 to 3000 cm⁻¹.
24 Results were obtained by averaging 256 scans with a resolution of 4 cm⁻¹.
25
26
27
28
29

30 *1-2. Computational methods*

31
32
33

34 **System description.** The silane molecules used are those presented in Table 1, after hydrolyzation,
35 based on a trisilanol structure with two silanol groups remaining unreacted to behave similarly to
36 a monofunctional silane (dimethylsilanol structure), as already reported in a previous study.²⁴ Such
37 a structure was used because its force field is already known¹⁸, whereas the force field of
38 dimethylsilanol is not published. The systems were built following the method proposed by
39 Roscioni *et al.*¹⁸ Silane molecules were initially randomly positioned on an amorphous SiO₂
40 surface, without explicit bonding between silane molecules and the surface, allowing their
41 spontaneous lateral organization. As surface roughness has a strong influence on the lateral
42 organization of silane molecules²⁵, the parameters of amorphous SiO₂ surface published by
43 Roscioni *et al.*¹⁸ were used. Indeed, its Root Mean Square (RMS) value is close to the experimental
44
45
46
47
48
49
50
51
52
53
54
55
56
57
58
59
60

1
2
3 value of SiO₂ thin films. Figure 1 illustrates the arrangement of the silane molecules on SiO₂
4 surface after 100-ns MD simulations. The simulation box included water molecules with the model
5 TIP4P. The charges of the silane head-groups were compensated with counterions (Na⁺ or Cl⁻) at
6 a concentration of 150 mM to mimic physiological conditions. A Lennard-Jones (LJ) wall was
7 added at the top of the box to avoid interactions between water and the bottom side of the SiO₂
8 surface and to prevent any surface curvature.²⁶ The simulation box included nearly 100 000 atoms
9 and its dimensions are 7.8 nm x 7.8 nm x 15 nm.
10
11
12
13
14
15
16
17
18
19
20
21
22
23
24
25
26
27
28
29
30
31
32
33
34
35
36
37
38
39
40
41
42
43
44
45
46
47
48
49
50
51
52
53
54
55
56
57
58
59
60

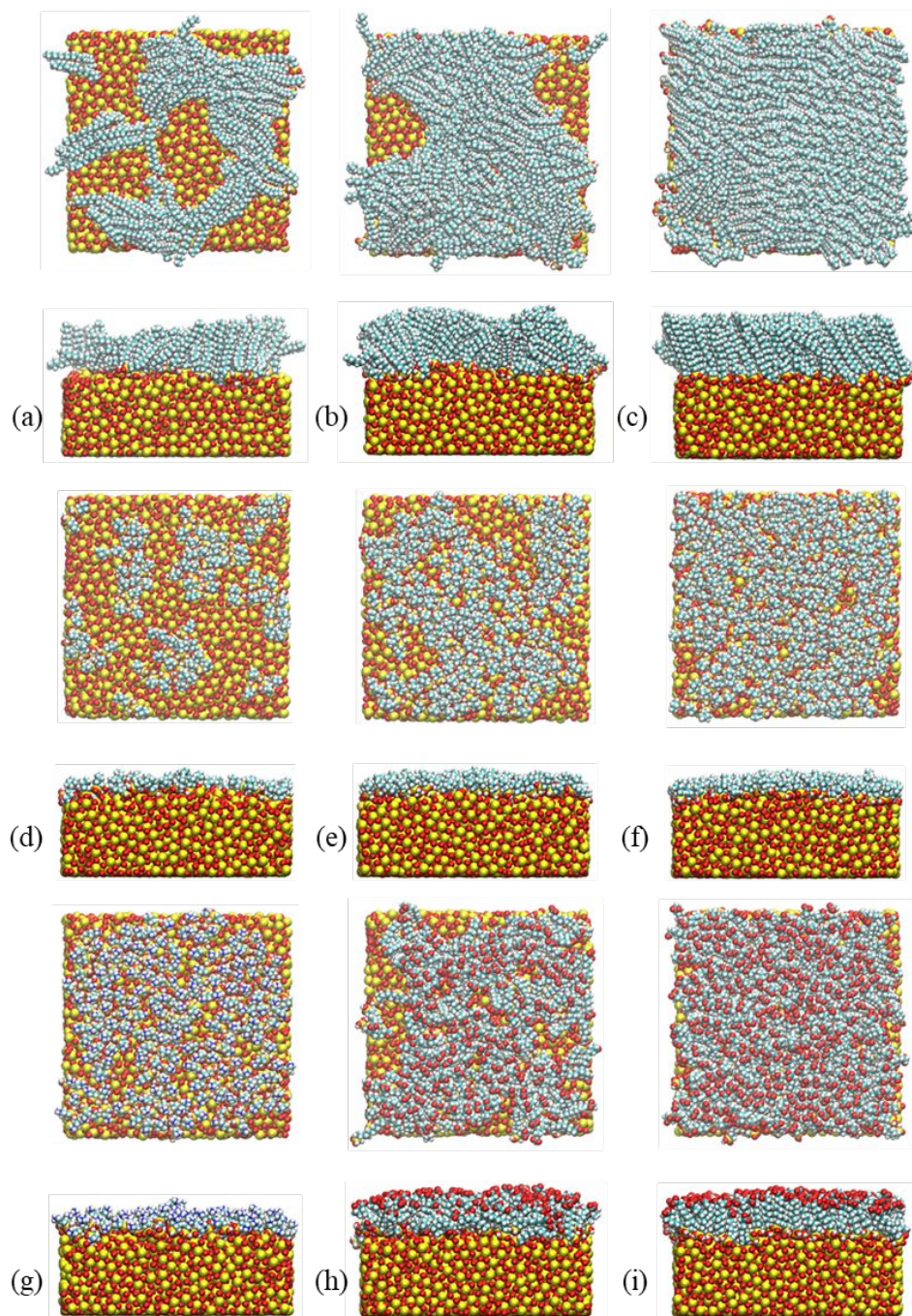


Figure 1. Arrangement of silane molecules on the amorphous SiO_2 layer after 100 ns MD simulation for different silane head-groups, alkyl chain lengths and surface coverages : (a) CH_3 long $c = 1.5 \text{ nm}^{-2}$, (b) CH_3 long $c = 3.0 \text{ nm}^{-2}$, (c) CH_3 long $c = 4.2 \text{ nm}^{-2}$, (d) CH_3 short $c = 1.5 \text{ nm}^{-2}$, (e) CH_3 short $c = 3.0 \text{ nm}^{-2}$, (f) CH_3 short $c = 4.2 \text{ nm}^{-2}$, (g) NH_3^+ $c = 3.0 \text{ nm}^{-2}$, (h) COO^- $c = 3.0$

1
2
3 nm⁻² and (i) COO⁻ c = 4.2 nm⁻². Atoms are shown in yellow (silicon), red (oxygen), cyan
4
5 (carbon), white (hydrogen) and blue (nitrogen).
6
7

8
9 **Simulation details.** All the simulations were performed with the Gromacs simulation package,
10 version 5.1.3²⁷ and the VMD software package version 1.9.3²⁸ was used for visualization. Firstly,
11 energy minimization was applied to the system using the Steepest Descent Minimization method.
12
13 Then, NVT and NPT equilibrations were carried during 100 ps each, and production simulations
14
15 were performed for 100 ns. A leap-frog algorithm was used for integration of the equations of
16
17 motion with a time step of 2 fs. Constraints were applied to bond parameters with a LINCS
18
19 algorithm. The temperature was maintained at 300 K with a Nose-Hoover thermostat using a time
20
21 constant of 0.4 ps and the pressure was kept at 1 bar with a Parrinello-Rahman barostat using a
22
23 time constant of 2 ps. Water and ions were both described with OPLS all-atom force-field.²⁹ The
24
25 parameters to describe the LJ wall were taken from a previous study.²⁶ Force-field for both silane
26
27 molecules and SiO₂ surfaces were adapted from recent studies^{18,19}, and from the OPLS²⁹ all-atom
28
29 force field. LJ potentials were truncated with a cut-off distance of 1 nm. Long range electrostatic
30
31 interactions were calculated with the Particle Mesh Ewald method and a cut-off of 1 nm.
32
33
34
35
36
37
38

39
40 **Analysis parameters.** The following parameters were evaluated by using Gromacs functions,
41
42 VMD tools and home-made Python codes. The errors bars were estimated using the standard
43
44 deviation. The curves and histograms were fitted using Bézier functions.
45
46

47
48 *Tilt angles.* The alkyl chain tilt angle is defined as the angle α between the normal to the SiO₂
49
50 surface and the vector between the silicon and terminal atoms of the silane molecule.¹⁸
51
52

53
54 *Gauche defects.* Gauche defect parameter was evaluated as the proportion of C-C-C-C torsion
55
56 angles in *trans* conformation.³⁰ For each silane molecule, we calculated all its C-C-C-C torsion
57
58
59
60

1
2
3 angle ϕ . If $150^\circ \leq \phi \leq 180^\circ$, the angle is in *trans* conformation and if $50^\circ \leq \phi \leq 150^\circ$, the angle is
4
5 in *gauche* conformation. Gauche defect parameter is the ratio r_{trans} between the number of *trans*
6
7 conformations and the total of *trans* and *gauche* conformations.
8
9

10
11 *Nematic order parameter.* The chemical bond order parameter S_2^i describes the orientation of the
12
13 i^{th} chemical bond, in a silane molecule, relative to the surface normal.³⁰ It is defined as:
14
15

$$16 \quad S_2^i = \frac{3 \cos^2 \varphi_i - 1}{2}$$

17
18
19
20
21 where φ_i is the angle between the i^{th} C-C bond and the surface normal. S_2^i takes values between -
22
23 0.5 and 1, where -0.5 corresponds to a bond parallel to the surface and 1 corresponds to a bond
24
25 perpendicular to the surface. We investigated the $\langle S_2^i \rangle$ value (average on all the silane molecules
26
27 of S_2^i values for a given i^{th} bond) and the S_2 distribution (probability of each S_2 value independently
28
29 of the bond number in the alkyl chain). In a group of randomly oriented bonds, $\langle S_2 \rangle = 0$ whereas
30
31 $\langle S_2^i \rangle = 0$ means that $\langle \varphi_i \rangle = 55^\circ$.
32
33
34
35
36

37 *Radial Distribution Function (RDF).* The 2D radial distribution of silane molecules was
38
39 investigated in the (x,y) plane (SiO_2 plane surface), taking into account periodic boundary
40
41 conditions. It is proportional to the probability of finding the Si atom of a silane neighboring
42
43 molecule for a given position on the plane, while the Si atom of the reference silane molecule is
44
45 fixed at origin.^{18,31}
46
47
48

49 **2. Results and Discussion**

50 *2.1 MD simulations*

Previous studies have shown the effects of alkyl chain length, with more than 6 carbon atoms ($n > 6$), at different surface coverages, on the structural properties of silane monolayers. In this study, we decipher the impact of charged functional head-group and alkyl chain length, with more than 3 carbon atoms ($n > 3$), at different surface coverages, on the structural properties of silane monolayers. MD simulations have been performed for all systems during 100 ns. The silane molecule diffusion distance is stabilized rapidly after 30 ns in all systems (Supporting information, Figure S1). After this diffusion phase, the Si atom of silane molecules can be considered as covalently fixed to the O atom of SiO₂. The alkyl chain tilt angle α , nematic order parameter $\langle S_2 \rangle$ and gauche defect fraction r_{trans} are correlated to the crystal packing of silane molecules. The results are summarized in Table 2.

Table 2. Alkyl chain tilt Angle, Nematic Order Parameter and Gauche Defect Parameter of the Silane Monolayers Studied.

System	Alkyl chain tilt angle ^(a)		Nematic order parameter $\langle S_2 \rangle$		Gauche defect parameter	
	α (°)	FWHM ^(b) (°)	Even bond	Odd bond	r_{trans}	
CH ₃ long	$c = 1.5 \text{ nm}^{-2}$	40	38	0.05	0.03	0.81
	$c = 3.0 \text{ nm}^{-2}$	34	26	0.06	0.22	0.85
	$c = 4.2 \text{ nm}^{-2}$	32	24	0.04	0.40	0.89
CH ₃ short	$c = 1.5 \text{ nm}^{-2}$	22	53	-0.04	0.32	(c)
	$c = 3.0 \text{ nm}^{-2}$	22	35	-0.04	0.42	(c)
	$c = 4.2 \text{ nm}^{-2}$	22	32	-0.03	0.53	(c)
NH ₃ ⁺	$c = 3.0 \text{ nm}^{-2}$	23	57	0.17	0.05	(c)
COO ⁻	$c = 3.0 \text{ nm}^{-2}$	19	27	0.20	0.16	0.69
	$c = 4.2 \text{ nm}^{-2}$	20	30	0.26	0.23	0.70

1
2
3 (a) Tilt angle distribution are depicted in Supporting Information, Figure S2. (b) Full Width at Half
4 Maximum (FWHM). (c) r_{trans} value is not relevant for small molecules with only one torsion angle.
5
6
7
8
9

10 **Tilt angle.** As shown in Table 2 (and Figure S2 in Supporting Information), the average tilt angle
11 of CH₃ long molecules increases from 32° to 40°, while the Full Width at Half Maximum (FWHM)
12 of the tilt angle distribution increases from 24° to 38°, as the surface coverage decreases from 4.2
13 nm⁻² to 1.5 nm⁻². This indicates that CH₃ long molecules straighten out and adopt a more organized
14 structure, as the coverage increases. These results are in agreement with previous MD studies, for
15 long alkyl chains ($n > 8$)¹⁸⁻²⁰, and can be explained by an increase in Van der Waals forces between
16 alkyl chains as their amount increases. However, very short alkyl chains (CH₃ short, NH₃⁺, $n = 3$)
17 seem to behave very differently from long ones ($n > 8$). The average tilt angles of NH₃⁺ and CH₃
18 short molecules seem to be independent of the studied surface coverages and they are similar,
19 around 20°. Furthermore, a charged head-group seems also to influence the tilt angle to surface
20 coverage relationship of silane molecules with long alkyl chains ($n > 8$). Indeed, despite a chain
21 length of eleven carbon atoms ($n = 11$), no influence of surface coverage was observed on the tilt
22 angle of COO⁻ silane molecules. Regarding on NH₃⁺ and COO⁻ molecules, repulsion between their
23 charged functional head-groups can explain the widening in their tilt angles distribution. The tilt
24 angle distribution of CH₃ short is larger than for CH₃ long, and the tilt angle distribution of NH₃⁺
25 is larger than for COO⁻ at a given surface coverage. It can be explained by the effect of Van der
26 Waals forces between long alkyl chains. These results suggest that the FWHM of tilt angle
27 distributions increases with charged head-groups and decreases as chain length increases.
28
29
30
31
32
33
34
35
36
37
38
39
40
41
42
43
44
45
46
47
48
49

50
51 Moreover, the degree of aggregation of silane molecules (observed on Figure 1), can be related to
52 the FWHM of the tilt angle distribution. Indeed, for a same coverage (*e.g.* $c = 3.0 \text{ nm}^{-2}$), CH₃ long
53
54
55
56
57
58
59
60

1
2
3 molecules are positioned within a single and dense aggregate, CH₃ short molecules form several
4 smaller aggregates separated by small non-functionalized SiO₂ areas, and silane molecules with
5 charged head-groups seem more evenly dispersed on the surface. So, both charged head-groups
6 and short alkyl chains seem to decrease silane molecule aggregation on the SiO₂ surface, while
7 increasing the FWHM of the tilt angle distributions. Indeed, the FWHM of the tilt angle is smaller
8 for CH₃ long monolayer (26°) than for CH₃ short (35°) and NH₃⁺ monolayers (57°) (Table 2).
9
10 Actually, silane molecules within a single dense aggregate could tend to behave similarly to
11 increase Van der Waals interactions (leading to a low FWHM value), while more evenly dispersed
12 silane molecules could be less impacted by the neighboring silane (leading to a high FWHM
13 value). However, COO⁻ and CH₃ long monolayers have similar FWHM (27° and 26° respectively),
14 despite very different surface distributions. This result could be explained by a balance between
15 the opposite effects of the charged head-group and of the long alkyl chain of COO⁻ molecules.
16
17
18
19
20
21
22
23
24
25
26
27
28
29

30
31 So, the FWHM of the tilt angle distribution of silane molecules seems to depend, in the same way
32 as the degree of dispersion of silane molecules on SiO₂ surface, on the presence of charged head-
33 groups and on the alkyl chain length.
34
35
36
37
38

39 **Gauche defects.** As shown in Table 2, CH₃ long silane molecules at low surface coverage ($c = 1.5$
40 nm^{-2}) present a lower r_{trans} , (0.81), which means that there are more gauche defects, than at higher
41 coverages ($r_{\text{trans}} = 0.85$ and $r_{\text{trans}} = 0.89$ for $c = 3.0 \text{ nm}^{-2}$ and $c = 4.2 \text{ nm}^{-2}$, respectively). These
42 findings are in good agreement with experimental reports found in the literature.^{22,32,33} COO⁻
43 molecules have more gauche defects than CH₃ long molecules for the same coverage ($r_{\text{trans}} = 0.69$
44 and $r_{\text{trans}} = 0.7$ for $c = 3.0 \text{ nm}^{-2}$ and $c = 4.2 \text{ nm}^{-2}$, respectively). The presence of charged head-
45 groups results in an increase in gauche defects. As the alkyl chains of NH₃⁺ and CH₃ short silane
46
47
48
49
50
51
52
53
54
55
56
57
58
59
60

1
2
3 molecules contain only one torsion angle, the calculation of their gauche defect parameter is not
4
5 relevant.
6

7
8 **Nematic order parameter.** As discussed above, in our CH₃ long monolayers, alkyl chains tilt
9 angles are in the range of 32° to 40°. As a consequence, for perfectly parallel CH₃ long molecules,
10 such angles should lead to S_2 values in the range of 0.98 to 1 for each odd bond and in the range
11 of -0.24 to -0.4 for each even bond. As the CH₃ long surface coverage increases, the odd bond
12 $\langle S_2^{2n+1} \rangle$ value increases from 0.03 to 0.4, as shown in Figure 2. Also, as shown in Figure 3, the S_2
13 probability distribution shows that two values for odd and even bonds (1 and -0.25) are more and
14 more represented as surface coverage increases. These results reveal that an organization of the
15 CH₃ long molecules in a herringbone structure appears as coverage increases, in agreement with
16 previous studies.^{18,22,30} Thus, long alkyl chains (without head-groups) and high surface coverage
17 lead to a well-ordered state, allowing a preferred alkyl chain orientation with few gauche
18 distortions. Regarding CH₃ short monolayers, alkyl chain tilt angles are around 22°. As a
19 consequence, for perfectly parallel CH₃ short molecules, such angles should lead to a S_2 value of
20 0.94 for the odd bond. Our results show that the CH₃ short odd bond $\langle S_2^1 \rangle$ value is 0.4 at $c = 3.0$
21 nm⁻² and 0.53 at $c = 4.2$ nm⁻², which is much higher than the odd bond $\langle S_2^{2n+1} \rangle$ values of CH₃ long
22 (respectively 0.2 and 0.4). Even if CH₃ short molecules have a large tilt angle distribution, the
23 order parameter relative to their second C-C bond is high, meaning that this C-C bond seems highly
24 ordered through the monolayer. In the case of NH₃⁺ and COO⁻ molecules, $\langle S_2^i \rangle$ values are close to
25 0 for even as well as for odd bonds, and the herringbone structure is not observed (Figure 2), even
26 at high coverage for COO⁻ molecules. All these observations suggest that the presence of charged
27 head-groups results in a more disordered monolayer.
28
29
30
31
32
33
34
35
36
37
38
39
40
41
42
43
44
45
46
47
48
49
50
51
52
53
54
55
56
57
58
59
60

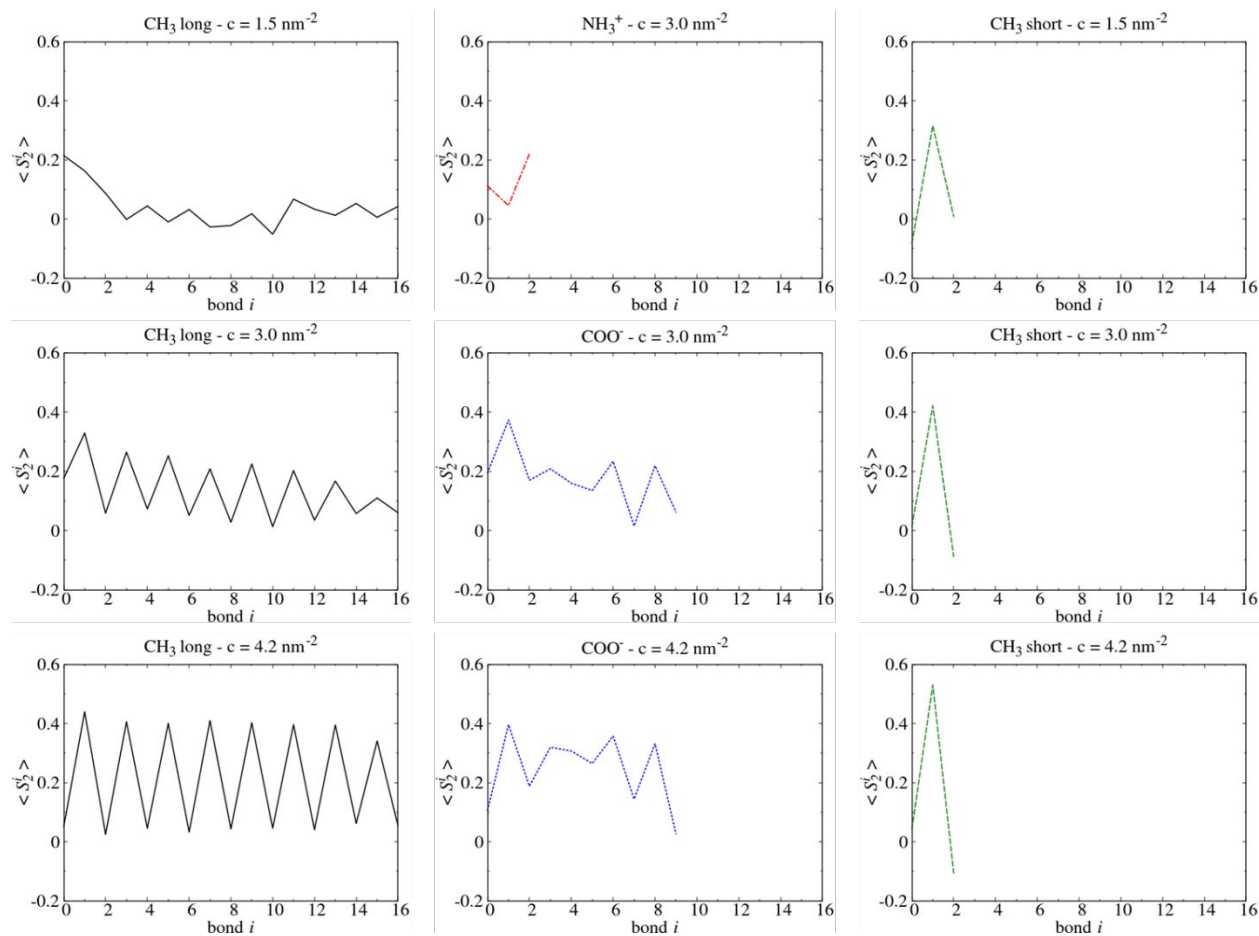
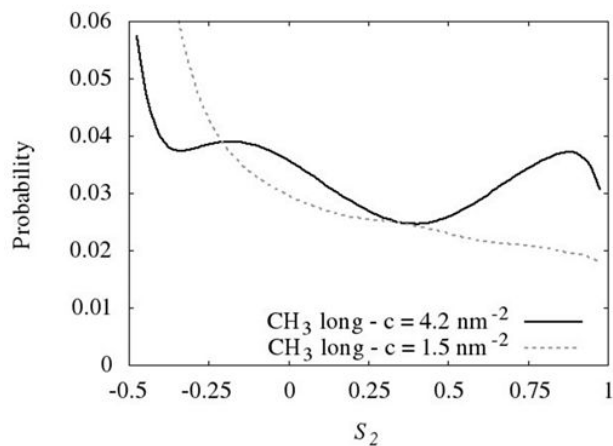


Figure 2. Average nematic order parameter $\langle S_2^i \rangle$ computed for each C-C or C-N bond of the different silane monolayers. Silane molecules present a herringbone structure when $\langle S_2^i \rangle$ varies periodically between odd and even bonds.



1
2
3 **Figure 3.** Distribution of the nematic order parameter S_2 for CH_3 long silane monolayer at
4 surface coverage $c = 1.5 \text{ nm}^{-2}$ and $c = 4.2 \text{ nm}^{-2}$. $S_2 = 0$ corresponds to a bond parallel to the
5 surface. For CH_3 long ($c = 4.2 \text{ nm}^{-2}$) values around -0.25 and 1 are more probable, which
6
7
8
9
10 corresponds to the S_2 values for a tilt angle of 32° .

11
12
13 **2D Radial Distribution Function.** The high nematic order parameters at high surface coverages
14 for CH_3 long suggest the presence of a positional order in these monolayers. To assess it, the two
15 dimensional Radial Distribution Function (RDF) in the (x,y) plane was calculated.^{18,34} At initial
16 state, because the silane molecules are randomly positioned in the (x,y) plane, the RDF is a line
17 whose slope is directly proportional to the surface coverage (Supporting Information, Figure S3).
18 At final state, all the systems present several peaks, which means that positional order and
19 periodicity appear even for the NH_3^+ silane molecules (Figure 4). As shown in Figure 5, for CH_3
20 long silane monolayers at $c = 3.0 \text{ nm}^{-2}$ and $c = 4.2 \text{ nm}^{-2}$, the 2D maps of the RDF clearly present a
21 hexagonal packing. This means that each silane molecule has six closest neighbors, spaced by 0.5
22 nm. For $c = 1.5 \text{ nm}^{-2}$, the hexagonal packing is less obvious and the intensity of the first peak
23 decreases. It can be explained by defects (absence of molecules at some places) in the monolayer
24 due to low surface coverage, as shown in Figure 1. These results are in agreement with previous
25 MD studies.^{18,34}

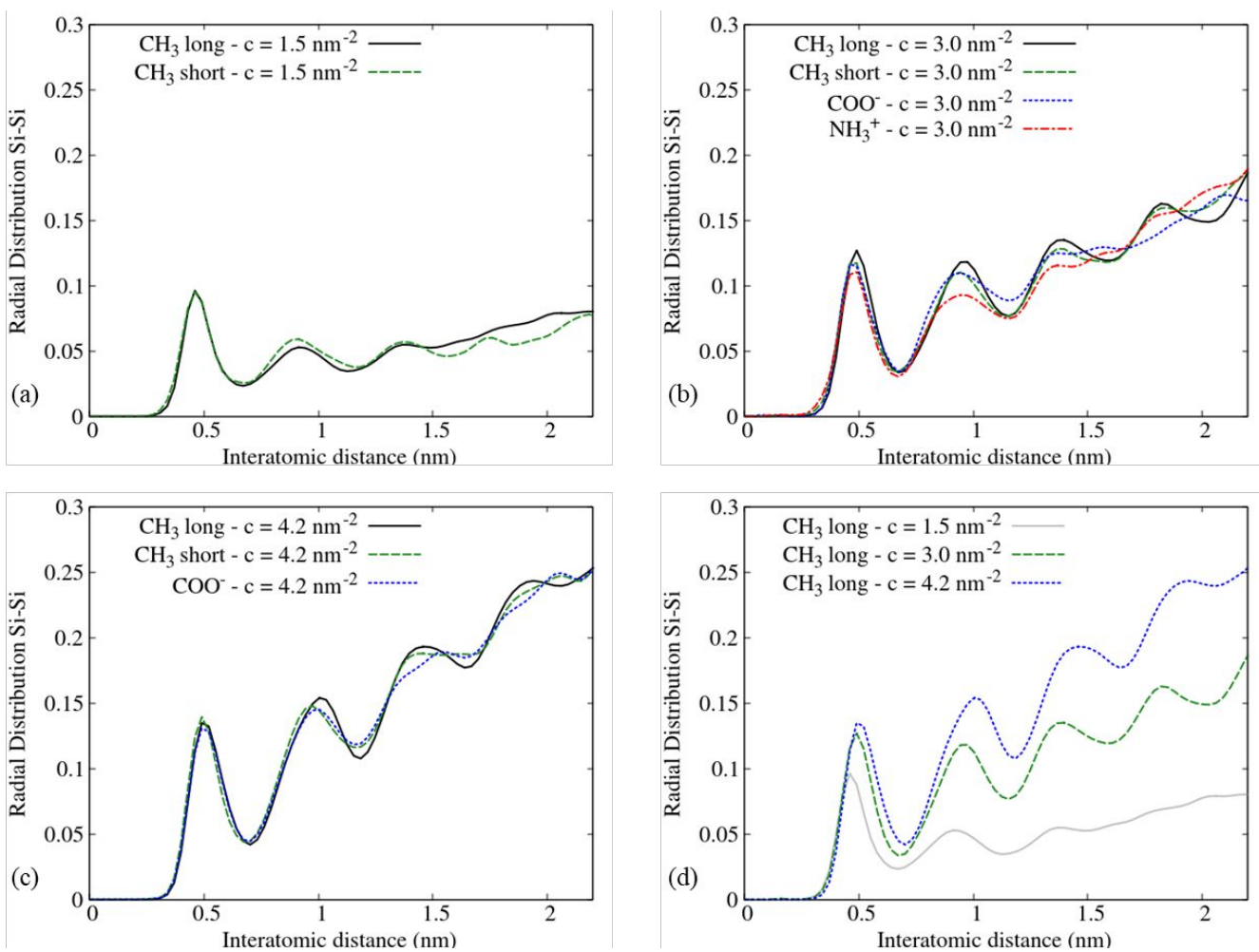


Figure 4. Radial distribution functions (RDF) of silane monolayers at different surface coverages: (a) $c = 1.5 \text{ nm}^{-2}$, (b) $c = 3.0 \text{ nm}^{-2}$, (c) $c = 4.2 \text{ nm}^{-2}$ and (d) CH_3 long at different coverages after 100 ns MD simulation. The peaks observed at a periodic interatomic distance show that a positional order appears in the silane monolayers.

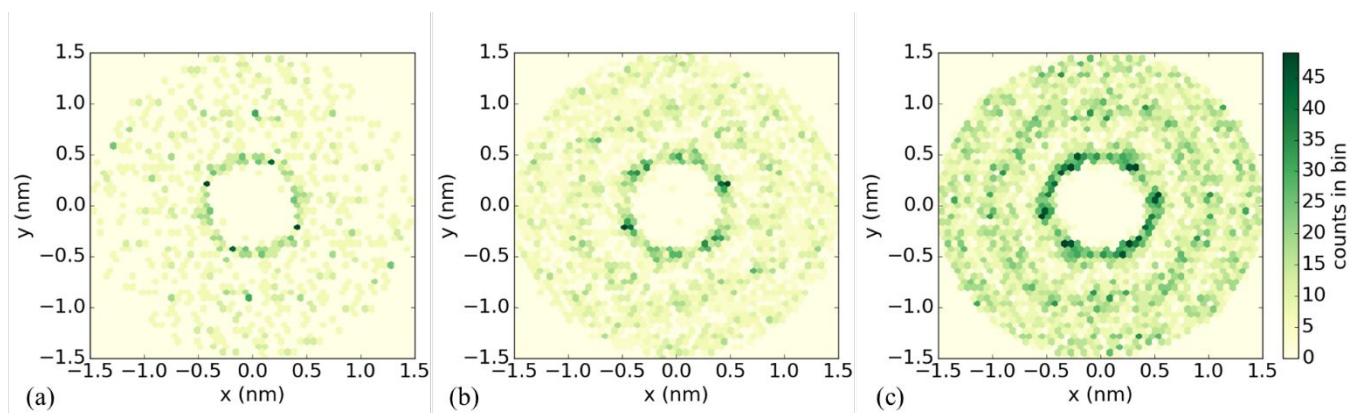


Figure 5. Two-dimensional Si – Si radial distribution functions of CH₃ long silane monolayer at different surface coverages (arbitrary units): (a) $c = 1.5 \text{ nm}^{-2}$, (b) $c = 3.0 \text{ nm}^{-2}$ and (c) $c = 4.2 \text{ nm}^{-2}$. A hexagonal positional order appears when surface coverage of alkylsilane molecules increases.

Moreover, our results show that, whatever the monolayer studied, independently of alkyl chain length and head-group charge, the first peak (*i.e.* lattice parameter, minimum Si-Si distance between two neighboring molecules) is shifted towards higher values as surface coverage increases, reaching 0.45 nm at $c = 1.5 \text{ nm}^{-2}$, 0.49 nm at $c = 3.0 \text{ nm}^{-2}$, and 0.5 nm at $c = 4.2 \text{ nm}^{-2}$. This result can be explained by the flexibility of the alkyl chains. Indeed, their higher flexibility at low surface coverage could allow Si atoms from silane molecules to position themselves closer to each other, during the diffusion phase of the MD simulation, while respecting the Van der Waals radius of the Si atom (which is 0.21 nm). For a given surface coverage, the intensity of the first peak is the same whatever the system. It means that the number of closest neighbor silane molecules does not depend on alkyl chain length and on charged head-groups. For CH₃ short and CH₃ long molecules at $c = 3.0 \text{ nm}^{-2}$ and $c = 4.2 \text{ nm}^{-2}$, the RDF shows that the hexagonal packing persists on the (x,y) plane, up to 2 nm around the origin as four peaks are well-defined on Figure 4. It is not the case for charged head-groups, only the two first peaks are visible meaning that the

1
2
3 propagation of the hexagonal packing is limited up to 1.5 nm. Consequently, NH_3^+ and COO^-
4 silane monolayers are more disordered than CH_3 short and CH_3 long monolayers.
5
6

7
8 To conclude, the persistence length of the hexagonal packing can be correlated with the nematic
9 order parameter, as it increases with surface coverage, it is independent of chain length and tilt
10 angle distribution, and it is prevented by charged head-groups. Thus, among the four investigated
11 silane monolayers, it seems that CH_3 long and CH_3 short monolayers at coverages $c = 3 \text{ nm}^{-2}$ and
12 $c = 4.2 \text{ nm}^{-2}$, lead to the highest positional order. However, CH_3 short silane molecules have a
13 larger tilt angle distribution than CH_3 long silane molecules. Also, the persistence length of the
14 hexagonal packing seems to be related to the degree of aggregation on the surface observed on
15 Figure 1. Indeed, for a coverage of 3.0 nm^{-2} , four peaks are well-defined on the RDF plots for CH_3
16 long and CH_3 short monolayers, while only two peaks are well-defined for NH_3^+ and COO^-
17 monolayers (Figure 4b). This result suggests that the persistence length of the hexagonal packing
18 increases with the degree of aggregation of silane molecules.
19
20
21
22
23
24
25
26
27
28
29
30
31
32

33 34 35 *2.2. Experimental validation of the simulated morphology*

36
37 Previous experimental studies have shown that molecules with long alkyl chains are more ordered,
38 they present smaller tilt angles, and are more densely packed on surface than molecules with short
39 alkyl chains.^{11,12,35-37} Most of the experimental studies are focused on multifunctional silane
40 molecules, allowing silane cross-linking, whereas in the MD simulations monofunctional silane
41 molecules are used. The monolayer morphology depends on the nature of silane molecules.³⁶ So,
42 to check that our simulation results are consistent with experiments, FTIR-ATR analysis were
43 carried out to qualitatively compare the alkyl chain tilt angle of the NH_3^+ , COO^- , CH_3 short and
44 CH_3 long monolayers. The surface coverages were estimated by XPS measurements.
45
46
47
48
49
50
51
52
53
54
55
56
57
58
59
60

XPS analysis. XPS survey spectra of the bare SiO₂/Aluminium/Silicon substrate, and of the four silanized SiO₂/Aluminium/Silicon substrates are shown on Figures S4 - S8 (Supporting Information). The bare substrate shows distinct O1s and Si2p peaks, while C1s is not detected. Silanized substrates show distinct C1s, O1s and Si2p peaks, their binding energies are reported in Table S1 (Supporting Information). C1s, O1s, and Si2p core levels are shown on Figure S5 – S8 (Supporting Information). Two contributions are present in the high resolution Si2p spectra for the silanized substrates, which are associated to Si(-O)₄ and to Si(-O)₁ (Table S1, Supporting Information). The Si(-O)₄ contribution is consistent with the silicon associated with oxygen in the silica substrate. The presence of Si(-O)₁ contribution comforts the success of the silanization. Indeed, the four silanes used in this study are monovalent. The atomic percentages of the bare substrate and of the four silanized substrates are reported in Table S1 (Supporting Information). The Si:O ratio is about 1.6 for each substrate. The Si(-O)₄:C ratio is consistent with the silane molecular composition, except for CH₃ short monolayer. Indeed, carbon contamination appears systematically on CH₃ short monolayer, although the silane solution is not contaminated.

The surface coverage of silanes, $\Gamma_{silanes}$, is estimated from the formula:³⁸

$$\Gamma_{silanes} = \frac{A_{Si(-O)_1}}{A_{Si2p}} n_{SiO_2} z$$

where $A_{Si(-O)_1}$ and A_{Si2p} are the normalized area of the Si(-O)₁ peak and of (Si(-O)₁ + Si(-O)₄) components respectively, n_{SiO_2} is the molecular concentration of silica (22 nm⁻³) and z is the sampling depth. z is approximated by 3λ , with λ is the mean free path in silica, equal to 3.7 nm.^{39,40} The surface coverages are about 3 nm⁻² for CH₃ short, CH₃ long, and COO⁻ monolayers, and around 8 nm⁻² for NH₃⁺. So, contrary to previous results obtained for multifunctional silanes¹², the

1
2
3 coverage does not depend on the alkyl chain length. The NH_3^+ surface coverage is more than two
4 times higher than the surface coverage obtained with the other silane molecules. It might be
5 explained by the catalytic effect of amino groups during silanization process.^{41,42} Also, it is worth
6 to be noticed that, because of sampling depth and variations in alkyl chain length, the calculation
7 underestimates the ratio between the surface coverage of short alkyl chains (CH_3 short or NH_3^+)
8 and long alkyl chains (CH_3 long or COO^-).
9
10
11
12
13
14
15
16
17

18 **FTIR-ATR analysis.** It is well-known that the methylene asymmetric stretching mode is shifted
19 to the lower frequency region as the alkyl chain order increases.^{11,17,43,44} Moreover, several studies
20 combining infrared spectroscopy, ellipsometry and AFM show that an increase in the alkyl chain
21 order, or a shift to lower frequency region, is associated with a decrease in the alkyl chain tilt
22 angle.^{12, 44}
23
24
25
26
27
28
29

30 The FTIR-ATR spectra of the COO^- , CH_3 long and NH_3^+ monolayers, shown in Figure 6, are
31 dominated by the methylene symmetric stretching mode (d^+ , in the range 2854 cm^{-1} - 2858 cm^{-1})
32 and the methylene asymmetric stretching (d^- , in the range 2924 cm^{-1} - 2928 cm^{-1}) mode. These
33 modes are not observed on the CH_3 short monolayer, likely because the CH_3 short molecule has
34 fewer methylene groups than the CH_3 long and COO^- molecules. However, despite NH_3^+ and CH_3
35 short molecules have the same number of methylene groups, d^+ and d^- modes are observed on the
36 NH_3^+ monolayer. It can be explained by the higher surface coverage obtained with NH_3^+ molecules
37 than with CH_3 short molecules (8 nm^{-2} vs. 3 nm^{-2}). Our results show a shift to low frequencies, by
38 up to 4 cm^{-1} , for d^- modes of CH_3 long (2929 cm^{-1}), NH_3^+ (2927 cm^{-1}), and COO^- (2925 cm^{-1})
39 monolayers. Such a shift suggests a higher tilt angle for CH_3 long than for NH_3^+ and COO^-
40 monolayers.⁴⁴ These results are in agreement with our tilt angles obtained by MD simulation.
41
42
43
44
45
46
47
48
49
50
51
52
53
54
55
56
57
58
59
60

of NH_3^+ molecules at a coverage of 4.2 nm^{-2} and the one of COO^- at a coverage of 3.0 nm^{-2} are close, around 12° - 19° (Supporting Information, Figure S2).

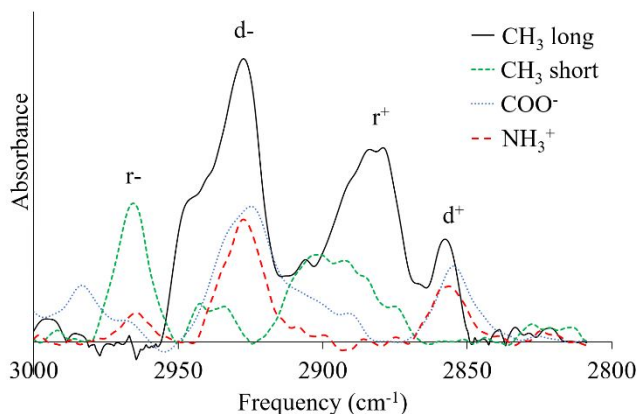


Figure 6. FTIR-ATR spectra of the four silanized surfaces.

The methyl asymmetric stretching mode (r^- in plane, 2966 cm^{-1}) is clearly resolved on the CH_3 short monolayer only, while the methyl symmetric stretching (r^+ , 2878 cm^{-1} and r^+ FR 2940 cm^{-1}) is clearly resolved on CH_3 long monolayer, but not on CH_3 short monolayer. Such results have already been observed from polarized FTIR-ATR experiments.¹² In polarized FTIR-ATR experiments, the r^- mode is observed only if the alkyl chains are nearly perpendicular to the surface, while the r^+ mode is observed for alkyl chains with higher tilt angles only. In the present study, we cannot calculate the different tilt angles because we use an unpolarized FTIR-ATR equipment. However, our results suggest that a change in orientation occurs between CH_3 long and CH_3 short molecules. Indeed as surface coverage is the same for CH_3 short and CH_3 long monolayers, if there were no change in the average alkyl chain tilt angle, then the r^- and r^+ peak areas of these two monolayers would be the same (with different widths, depending on the tilt angle distribution). By assuming that the presence of the r^- mode on the CH_3 short system is not entirely linked to the carbon contamination, these experimental results are qualitatively in agreement with tilt angles

1
2
3 from our MD simulations, which suggest that the tilt angle of CH₃ long molecules is 34° while the
4
5 one of CH₃ short molecules is 22°.
6
7

8
9 Previous experimental studies have shown that, in the case of multifunctional silane molecules,
10
11 the surface coverage increases, and the tilt angle decreases, as the alkyl chain length increases.¹²
12
13 Our experimental and simulated results suggest that, in the case of monofunctional silane
14
15 molecules, likely because of the absence of intermolecular bonds, the alkyl chain length has no
16
17 significant effect on the surface coverage. However, the average chain tilt angle increases as the
18
19 chain length increases.
20
21
22

23 **3. Conclusion**

24
25
26 This study shows that the ordered state of the silane monolayer depends on the alkyl chain length
27
28 (n from 3 to 18), head-group charge, and on the surface coverage. Indeed, long alkyl chains and
29
30 high coverages lead to more organized self-assembled silane monolayers, with a narrow tilt angle
31
32 distribution centered on a preferred orientation, and few gauche distortions. Also, for given alkyl
33
34 chain length and surface coverage, charged silane molecules lead to a more disordered state than
35
36 neutral silane molecules, with a larger tilt angle distribution. Long alkyl chains ($n > 8$) were
37
38 reported to have a tilt angle independent of chain length and to be affected by surface coverage.
39
40 On the contrary, short alkyl chains ($n = 3$) behave very differently, since their tilt angle seems to
41
42 be independent from surface coverage. Furthermore, a charged head-group seems to influence the
43
44 tilt angle to surface coverage relationship of long alkyl chain ($n > 8$). Indeed no influence of surface
45
46 coverage on the COO⁻ ($n = 11$) tilt angle was observed. The differences between the simulated tilt
47
48 angles, depending on the nature of silane molecules, are validated by FTIR-ATR analysis.
49
50
51
52
53
54
55
56
57
58
59
60

1
2
3 Moreover, our results suggest that a hexagonal packing is observed in all the studied silane
4 monolayers. However, whatever the alkyl chain length, an increase in surface coverage lead to the
5 more marked appearance of the hexagonal packing. Nematic order parameter values show that
6 such packing is governed by the parallel orientation of the first C-C bonds of the silane molecules,
7 near the SiO₂ surface. Thus, even short alkyl chain (CH₃ short), despite a large tilt angle
8 distribution, present a well-defined hexagonal packing at high coverage.
9

10
11
12 Surface chemical functionalization is used in analytical tools as a mean to immobilize
13 biomolecules that will capture a specific analyte, but also to reduce the non-specific adsorption.
14
15 This work could further help to understand the influence of the nature of silane molecules on the
16 arrangement of the silane monolayer on SiO₂ surfaces, and on subsequent biomolecule
17 interactions, to design more efficient analytical tools.
18
19
20
21
22
23
24
25
26
27
28
29
30
31

32 ASSOCIATED CONTENT

33
34
35
36 The following files are available free of charge.

37
38
39 Diffusion distance of silane molecules. Tilt angle distributions. Sub-coverages for each system
40 studied at 3 nm⁻² and 1.5 nm⁻². Radial distribution functions of CH₃ long silane molecules. XPS
41 spectra. XPS binding energy and atomic percentages. (PDF)
42
43
44
45
46

47 AUTHOR INFORMATION

48 49 50 **Corresponding Author**

51
52
53 *Email: christelle.yeromonahos@ec-lyon.fr
54
55
56
57
58
59
60

Author Contributions

The manuscript was written through contributions of all authors. All authors have given approval to the final version of the manuscript.

Funding Sources

This work was supported by the Young Researcher ANR PORIDG project, grant ANR-18-CE09-0006 of the French Agence Nationale de la Recherche. This work was granted access to the HPC resources of CINES under the allocation 2019-A0070711100 made by GENCI. Also, this work was supported by the PMCS2I - supercomputer Newton from Ecole Centrale de Lyon, France, member of the FLMSN.

ACKNOWLEDGMENT

The authors thank Laurent Pouilloux, Anne Cadiou, and Laurent Carrel for support on PMCS2I resources.

REFERENCES

- (1) Beaucage, S. L. Strategies in the preparation of DNA oligonucleotide arrays for diagnostic applications. *Curr. Med. Chem.* **2001**, *8*, 1213-1244.
- (2) Beier, M.; Hoheisel, J. D. Versatile derivatisation of solid support media for covalent bonding on DNA-microchips. *Nucleic Acids Res.* **1999**, *27*, 1970-1977.
- (3) Wang, Y.; Cai, J.; Rauscher, H.; Behm, R. J.; Goedel, W. A. Maleimido-Terminated Self-Assembled Monolayers. *Chem. Eur. J.* **2005**, *11*, 3968-3978.

- 1
2
3 (4) Luderer F.; Walschus U. Immobilization of Oligonucleotides for Biochemical Sensing by Self-
4 Assembled Monolayers: Thiol-Organic Bonding on Gold and Silanization on Silica Surfaces.
5
6 Wittmann C. (eds) *Immobilisation of DNA on Chips I. Topics in Current Chemistry Springer,*
7
8 *Berlin Heidelberg* **2005**, 260, 37-56.
9
10
11
12
13 (5) Hitaishi, V. P. ; Clement, R. ; Bourassin, N. ; Baaden, M. ; De Poulpiquet, A. ; Sacquin-Mora,
14
15 S. ; Ciaccafava, A. ; Lojou, E. Controlling redox enzyme orientation at planar electrodes. *Catalysts*
16
17 **2018**, 8, 192.
18
19
20
21 (6) Ruan, M.; Seydou, M.; Noel, V.; Piro, B.; Maurel, F.; Barbault, F. Molecular dynamics
22
23 simulation of a RNA aptasensor. *J. Phys. Chem. B* **2017**, 121, 4071-4080.
24
25
26 (7) Chu-jiang, C.; Zhi-gang, S.; Yu-shan, X.; Shu-lin, M. Surface topography and character of γ -
27
28 aminopropyltriethoxysilane and dodecyltrimethoxysilane films adsorbed on the silicon dioxide
29
30 substrate via vapour phase deposition. *J. Phys. D: Appl. Phys.* **2006**, 39, 4829-4837.
31
32
33
34 (8) Halliwell, C. M.; Cass, A. E. A factorial analysis of silanization conditions for the
35
36 immobilization of oligonucleotides on glass surfaces. *Anal. Chem.* **2001**, 73, 2476-2483.
37
38
39
40 (9) Al-Hajj, N.; Mousli, Y.; Miche, A.; Humblot, V.; Hunel, J.; Heuzé, K.; Buffeteau, T.; Genin,
41
42 E.; Vellutini, L. Influence of the Grafting Process on the Orientation and the Reactivity of Azide-
43
44 Terminated Monolayers onto Silica Surface. *Appl. Surf. Sci.* **2020**, 146778.
45
46
47 (10) Britt, D. W.; Hlady, V. An AFM study of the effects of silanization temperature, hydration,
48
49 and annealing on the nucleation and aggregation of condensed OTS domains on mica. *J. Colloid*
50
51 *Interface Sci.* **1996**, 178, 775-784.
52
53
54
55
56
57
58
59
60

1
2
3 (11) Yeon, H.; Wang, C.; Van Lehn, R. C.; Abbott, N. L. Influence of Order within Nonpolar
4 Monolayers on Hydrophobic Interactions. *Langmuir* **2017**, *33*, 4628-4637.

5
6
7
8
9 (12) Barrett, A.; Petersen, P. B. Order of dry and wet mixed-length self-assembled monolayers. *J.*
10 *Phys. Chem. C* **2015**, *119*, 23943-23950.

11
12
13
14 (13) Steinrück, H. G.; Will, J.; Magerl, A.; Ocko, B. M. Structure of n-Alkyltrichlorosilane
15 Monolayers on Si (100)/SiO₂. *Langmuir* **2015**, *31*, 11774-11780.

16
17
18
19
20 (14) Wen, K.; Maoz, R.; Cohen, H.; Sagiv, J.; Gibaud, A.; Desert, A.; Ocko, B. M. Postassembly
21 chemical modification of a highly ordered organosilane multilayer: New insights into the structure,
22 bonding, and dynamics of self-assembling silane monolayers. *ACS nano* **2008**, *2*, 579-599.

23
24
25
26
27
28 (15) Koga, T.; Honda, K.; Sasaki, S.; Sakata, O.; Takahara, A. Phase transition of alkylsilane
29 monolayers studied by temperature-dependent grazing incidence X-ray diffraction. *Langmuir*
30 **2007**, *23*, 8861-8865.

31
32
33
34
35
36 (16) Ito, Y.; Virkar, A. A.; Mannsfeld, S.; Oh, J. H.; Toney, M.; Locklin, J.; Bao, Z. Crystalline
37 ultrasmooth self-assembled monolayers of alkylsilanes for organic field-effect transistors. *J. Am.*
38 *Chem. Soc.* **2009**, *131*, 9396-9404.

39
40
41
42
43 (17) Naik V.V.; Städler R.; Spender N.D. Effect of leaving group on the structures of alkylsilane
44 SAMs. *Langmuir* **2014**, *30*, 14824-14831.

45
46
47
48
49 (18) Roscioni, O. M.; Muccioli, L.; Mityashin, A.; Cornil, J.; Zannoni, C. Structural
50 characterization of alkylsilane and fluoroalkylsilane self-assembled monolayers on SiO₂ by
51 molecular dynamics simulations. *J. Phys. Chem. C* **2016**, *120*, 14652-14662.

1
2
3 (19) Castillo, J. M.; Klos, M.; Jacobs, K.; Horsch, M.; Hasse, H. (2015). Characterization of
4 alkylsilane self-assembled monolayers by molecular simulation. *Langmuir* **2015**, *31*, 2630-2638.
5
6

7
8
9 (20) Black, J. E.; Iacovella, C. R.; Cummings, P. T.; McCabe, C. Molecular dynamics study of
10 alkylsilane monolayers on realistic amorphous silica surfaces. *Langmuir* **2015**, *31*, 3086-3093.
11
12

13
14 (21) Black, J. E.; Summers, A. Z.; Iacovella, C. R.; Cummings, P. T.; McCabe, C. Investigation
15 of the Impact of Cross-Polymerization on the Structural and Frictional Properties of Alkylsilane
16 Monolayers Using Molecular Simulation. *Nanomaterials* **2019**, *9*, 639.
17
18

19
20 (22) Ewers, B.W.; Batteas, J.D. Molecular dynamics simulations of alkylsilane monolayers on
21 silica nanoasperities: impact of surface curvature on monolayer structure and pathways for energy
22 dissipation in tribological contacts. *J. Phys. Chem. C* **2012**, *116*, 25165-25177.
23
24
25
26

27
28 (23) Dugas, V.; Depret, G.; Chevalier, Y.; Nesme, X.; Souteyrand, É. Immobilization of single-
29 stranded DNA fragments to solid surfaces and their repeatable specific hybridization: covalent
30 binding or adsorption? *Sens. Actuator B-Chem.* **2004**, *101*, 112-121.
31
32
33
34

35
36 (24) Lecot S.; Chevolut Y.; Phaner-Goutorbe M.; Yeromonahos C. Impact of silane monolayers
37 on the adsorption of streptavidin on silica and its subsequent interactions with biotin: molecular
38 dynamics and steered molecular dynamics simulations. *J. Phys. Chem. B* **2020**, *124*, 6786-6796.
39
40
41
42

43
44 (25) Roscioni, O. M.; Muccioli, L.; Della Valle, R. G.; Pizzirusso, A.; Ricci, M.; Zannoni, C.
45 Predicting the anchoring of liquid crystals at a solid surface: 5-cyanobiphenyl on cristobalite and
46 glassy silica surfaces of increasing roughness. *Langmuir* **2013**, *29*, 8950-8958.
47
48
49
50

51
52 (26) Kitabata, M.; Taddese, T.; Okazaki, S. Molecular dynamics study on wettability of poly
53 (vinylidene fluoride) crystalline and amorphous surfaces. *Langmuir* **2018**, *34*, 12214-12223.
54
55
56
57

1
2
3 (27) Van Der Spoel, D.; Lindahl, E.; Hess, B., Groenhof, G.; Mark, A. E.; Berendsen, H. J.
4 GROMACS: fast, flexible, and free. *J. Comput. Chem.* **2005**, *26*, 1701-1718.
5
6

7
8 (28) Humphrey, W.; Dalke, A.; Schulten, K. VMD: visual molecular dynamics. *J. Mol. Graph.*
9 **1996**, *14*, 33-38.
10
11

12
13 (29) Jorgensen, W. L.; Maxwell, D. S.; Tirado-Rives, J. Development and testing of the OPLS all-
14 atom force field on conformational energetics and properties of organic liquids. *J. Am. Chem. Soc.*
15 **1996**, *118*, 11225-11236.
16
17
18

19
20 (30) Schulze, E.; Stein, M. Simulation of Mixed Self-Assembled Monolayers on Gold: Effect of
21 Terminal Alkyl Anchor Chain and Monolayer Composition. *J. Phys. Chem. B* **2018**, *122*, 7699-
22 7710.
23
24
25
26
27

28
29 (31) Anvari, M. H.; Liu, Q.; Xu, Z.; Choi, P. Molecular Dynamics Study of Hydrophilic Sphalerite
30 (110) Surface as Modified by Normal and Branched Butylthiols. *Langmuir* **2018**, *34*, 3363-3373.
31
32
33

34
35 (32) Parikh, A. N.; Allara, D. L.; Azouz, I. B.; Rondelez, F. An intrinsic relationship between
36 molecular structure in self-assembled n-alkylsiloxane monolayers and deposition temperature. *The*
37 *J. Phys. Chem.* **1994**, *98*, 7577-7590.
38
39
40
41

42
43 (33) Allara, D. L.; Nuzzo, R. G. Spontaneously organized molecular assemblies. 2. Quantitative
44 infrared spectroscopic determination of equilibrium structures of solution-adsorbed n-alkanoic
45 acids on an oxidized aluminum surface. *Langmuir* **1985**, *1*, 52-66.
46
47
48
49

50
51 (34) Deetz, J. D.; Ngo, Q.; Faller, R. Reactive Molecular Dynamics Simulations of the Silanization
52 of Silica Substrates by Methoxysilanes and Hydroxysilanes. *Langmuir* **2016**, *32*, 7045-7055.
53
54
55
56
57
58
59
60

- 1
2
3 (35) Porter, M. D.; Bright, T. B.; Allara, D. L.; Chidsey, C. E. Spontaneously organized molecular
4 assemblies. 4. Structural characterization of n-alkyl thiol monolayers on gold by optical
5 ellipsometry, infrared spectroscopy, and electrochemistry. *J. Am. Chem. Soc.* **1987**, *109*, 3559-
6 3568.
7
8
9
10
11
12
13 (36) Ulman, A. Formation and structure of self-assembled monolayers. *Chem. Rev.* **1996**, *96*,
14 1533-1554.
15
16
17
18 (37) Pujari, S. P.; Scheres, L.; Marcelis, A. T. ; Zuilhof, H. Covalent surface modification of oxide
19 surfaces. *Angew. Chem. Int. Ed.* **2014**, *53*, 6322-6356.
20
21
22
23
24 (38) Shircliff, R. A.; Martin, I. T.; Pankow, J. W.; Fennell, J.; Stradins, P.; Ghirardi, M. L.; Cowley,
25 S. W.; Branz, H. M. High-resolution X-ray photoelectron spectroscopy of mixed silane monolayers
26 for DNA attachment. *ACS Appl. Mater. Interfaces* **2011**, *3*, 3285-3292.
27
28
29
30
31 (39) Vickerman, J. C.; Gilmore, I. S. (Eds.) Surface analysis: the principal techniques. *John Wiley*
32 *& Sons.* **2011**.
33
34
35
36
37 (40) Tanuma, S.; Powell, C. J.; Penn, D. R. Calculations of electron inelastic mean free paths
38 (IMFPS). IV. Evaluation of calculated IMFPS and of the predictive IMFPS formula TPP-2 for
39 electron energies between 50 and 2000 eV. *Surf. Interface Anal.* **1993**, *20*, 77-89.
40
41
42
43
44 (41) Kinkel, J. N.; Unger, K. K. Role of solvent and base in the silanization reaction of silicas for
45 reversed-phase high-performance liquid chromatography. *J. Chromatogr. A*, **1984**, *316*, 193-200.
46
47
48
49
50 (42) Fadeev, A. Y.; McCarthy, T. J. Self-assembly is not the only reaction possible between
51 alkyltrichlorosilanes and surfaces: monomolecular and oligomeric covalently attached layers of
52 dichloro- and trichloroalkylsilanes on silicon. *Langmuir* **2000**, *16*, 7268-7274.
53
54
55
56
57
58
59
60

(43) Ardès-Guisot, N.; Durand, J. O.; Granier, M.; Perzyna, A.; Coffinier, Y.; Grandidier, B.; Wallart X.; Stievenard, D. Trichlorosilane isocyanate as coupling agent for mild conditions functionalization of silica-coated surfaces. *Langmuir* **2005**, *21*, 9406-9408.

(44) Nam, H.; Granier, M.; Boury, B.; Park, S.Y. Functional organotrimethoxysilane derivative with strong intermolecular $\pi-\pi$ interaction: One-pot grafting reaction on oxidized silicon substrates. *Langmuir* **2006**, *22*, 7132-7134.

For Table of Contents Only

